The tiliroside derivative, 3-*O*-[(*E*)-(2-oxo-4-(p-tolyl) but-3-en-1-yl] kaempferol produced inhibition of neuroinflammation and activation of AMPK and Nrf2/HO-1 pathways in BV-2 microglia

Ravikanth Velagapudi[a,c], Faisal Jamshaid[b,d], Izabela Lepiarz[a], Folashade O Katola[a], Karl Hemming[b], Olumayokun A Olajide[a]

[a] Department of Pharmacy, School of Applied Sciences, University of Huddersfield, Huddersfield, United Kingdom

[b] Department of Chemical Sciences, School of Applied Sciences, University of Huddersfield, Huddersfield, United Kingdom

[c] Current Address: Center for Translational Pain Medicine, Department of Anesthesiology, Duke University Medical Center, Durham, NC, 27710, USA

[d] Current Address: 1018 Liaohe Road, Xinbei Zone, Changzhou, Jiangsu, China

***Author for Correspondence**

Dr Olumayokun A Olajide

Department of Pharmacy, School of Applied Sciences

University of Huddersfield

Queensgate, Huddersfield, HD1 3DH

United Kingdom

Email: o.a.olajide@hud.ac.uk

Telephone: +44 (0) 1484 472735

Abstract

Neuroinflammation is now widely accepted as an important pathophysiological mechanism in neurodegenerative disorders, thus providing a critical target for novel compounds. In this study, 3-O-[(E)-(2-oxo-4-(p-tolyl) but 3 en 1 yl] kaempferol (OTBK) prevented the production of pro-inflammatory mediators TNFα, IL-6, PGE_2 and nitrite from BV-2 microglia activated with LPS and IFNγ. These effects were accompanied by a reduction in the levels of pro-inflammatory proteins COX-2 and iNOS. Involvement of NF-κB in the anti-inflammatory activity of OTBK was evaluated in experiments showing that the compound prevented phosphorylation, nuclear accumulation and DNA binding of p65 sub-unit induced by stimulation of BV-2 microglia with LPS and IFNγ. Exposure of mouse hippocampal HT22 neurons to conditioned media from LPS + IFNγ-stimulated BV-2 cells resulted in reduced cell viability and generation of cellular reactive oxygen species. Interestingly, conditioned media from LPS/IFNγ-stimulated BV-2 cells which were treated with OTBK did not induce neuronal damage or oxidative stress. OTBK was shown to increase protein levels of phospho-AMPKα, Nrf2 and HO-1 in BV-2 microglia. It was further revealed that OTBK treatment increased Nrf2 DNA binding in BV-2 microglia. The actions of the compound on AMPKα and Nrf2 were shown to contribute to its anti-inflammatory activity as demonstrated by diminished activity in the presence of the AMPK antagonist dorsomorphin and Nrf2 inhibitor trigonelline. These results suggest that OTBK inhibits neuroinflammation through mechanisms that may involve activation of AMPKα and Nrf2 in BV-2 microglia.

Keywords:

3-*O*-[(*E*)-(2-oxo-4-(p-tolyl)-but-3-en-1-yl] kaempferol; Anti-inflammatory; Microglia; AMPKα; Nrf2; Neuroprotection

1. Introduction

Neuroinflammation by the immune system in the brain is an important process in the understanding of neurobiology and therapeutics of neurodegenerative disorders such as Alzheimer's disease (AD) [1, 2] and Parkinson's disease (PD) [3]. Neuroinflammation involves a sustained activation of macrophages in the brain, known as microglia resulting in the secretion of neurotoxic factors, including pro-inflammatory cytokines, chemokines and reactive oxygen species (ROS). Consequently, attention is now focused on the synthesis of novel anti-inflammatory agents with neuroprotective potential for AD therapeutics.

Adenosine monophosphate-activated protein kinase (AMPK) is a protein kinase that plays a critical role in regulating energy metabolism. Studies have suggested that activating AMPK produces anti-inflammatory activity through indirect inhibition of NF-κB. In neuroinflammation, AMPK activation has been proposed to have beneficial effects [4]. For example, ENERGI-F704 a known AMPK activator was shown to inhibit neuroinflammation in LPS-stimulated BV-2 microglia by preventing nuclear translocation and protein levels of NF-κB with the subsequent reduction in IL-6, TNFα, iNOS and COX-2 [5].

The Nrf2 activation pathway is an emerging drug target for the treatment of neurodegenerative disorders such as AD and PD due to its ability to suppress neuroinflammation. Reports have shown that Nrf2 activation results in inhibition of neuroinflammation through transcriptional repression of pro-inflammatory cytokines such as TNFα, IL-1, and IL-6 in microglia [6]. Furthermore, the Nrf2 activator sulphoraphane has been reported to enhance Nrf2 DNA-binding activity as well as inducing upregulation of Nrf2 target genes in the microglia, while inhibiting LPS-induced interleukin IL-1β, IL-6, and iNOS production [7].

Previously we reported that tiliroside, a dietary glycosidic flavonoid inhibited neuroinflammation in LPS-activated BV-2 microglia through multiple mechanisms involving NF-κB, p38 MAPK and Nrf2 activation pathways [8, 9]. Interestingly, a novel tiliroside derivative, 3-*O*-[(*E*)-(2-oxo-4-(p-tolyl)but-3-en-1-yl] kaempferol (OTBK) (Figure 1) has been shown to enhance glucose consumption by insulin-resistant HepG2 cells [10]. In experiments reported by Shi et al. (2011), a closely related compound to OTBK increased GLUT4 translocation in muscle cells through a

mechanism linked to AMPK activation [11]. In this study we have investigated effects of OTBK in BV-2 microglia to determine whether it would inhibit neuroinflammation. We have also evaluated the roles of Nrf2 and AMPK activation in the anti-inflammatory activity of the compound.

2. Materials and methods

2.1 Synthesis of 3-*O*-[(*E*)-(2-oxo-4-(p-tolyl) but-3-en-1-yl] kaempferol (OTBK)

OTBK was synthesised from the reaction of kaempferol with freshly prepared (*E*)-1-bromo-4-(p-tolyl) but-3-en-2-one [12], in the presence of potassium carbonate in boiling dioxane (Supplementary Data 1). After 48 h, silica gel chromatographic work-up gave a 34% yield of the pure desired product compared to the 13.4% yield reported previously [10]. Lipopolysaccharide (LPS) derived from *Salmonella enterica* serotype *typhimurium* SL1181 (Sigma) was used in these experiments at a concentration of 100 ng/ml. Interferon (IFNγ) derived from *E. coli* (R and D Systems) was used at a concentration of 5 ng/ml. In all cases, cells were treated with OTBK 30 min prior to stimulation with LPS and IFNγ.

2.2 Cell culture

BV-2 mouse microglia cell line ICLC ATL03001 (Interlab Cell Line Collection, Banca Biologica e Cell Factory, Italy) were cultured in RPMI1640 medium (Gibco). HEK293 (ATCC CRL 1573) cells were obtained from the European Collection of Cell Cultures (Salisbury, UK) and were cultured in MEM-eagle's medium (Gibco). HT22 mouse hippocampal neurons were a kind gift from Dr Jeff Davis and were cultured in DMEM (Gibco). All culture media were supplemented with 10% fetal bovine serum, 2 mM L-glutamine, 1 mM sodium pyruvate, 100 U/ml penicillin and 100 mg/ml streptomycin.

2.3 Determination of pro-inflammatory cytokines, nitrite and PGE_2 in LPS + IFNγ-activated BV-2 microglia

This was carried out as described earlier [13, 14]. BV-2 microglia were treated with OTBK (2.5, 5 and 10 μM) 30 min prior to stimulation with LPS (100 ng/ml) and IFNγ (5 ng/ml) for a further 24 h. Levels of TNFα and IL-6 in culture supernatants were determined using mouse TNFα and IL-6 ELISA kits (Biolegend, UK), while nitrite production was measured using the Griess assay kit (Promega, UK). Levels of PGE2 were measured using PGE_2 EIA kit (Arbor Assays, USA).

Culture medium in HT22 hippocampal neurons cells were completely removed and replaced with conditioned media (200 µl) from LPS + IFNγ-stimulated BV-2 cells This was incubated for a further 24 h in 5% CO_2 at 37°C. Neuronal viability was determined using MTT cell viability assay, while cellular ROS generation in the neurons was measured using the fluorescence DCFDA method assay kit (Abcam).

2.4 Immunoblotting

Following treatment, microglia cell lysates were prepared by washing cells with PBS, followed by addition of lysis buffer and phenylmethylsulfonyl fluoride (PMSF), and centrifugation for 10 min. Nuclear extracts were prepared using EpiSeeker Nuclear Extraction Kit (Abcam) according to the manufacturer's instructions.

Twenty-five micrograms of protein was subjected to sodium dodecyl sulfate polyacrylamide (SDS) gel electrophoresis. Proteins were then transferred to polyvinylidene fluoride (PVDF) membranes (Millipore, Bedford, MA, USA) for 2 h. Membranes were then blocked at room temperature for 1 h and then incubated with primary antibodies overnight at 4°C. Primary antibodies used in the experiments were rabbit anti-HO-1 (Santa Cruz; 1:500), rabbit anti-COX-2 (Santa Cruz; 1:500), rabbit anti-iNOS (Santa Cruz; 1:500), rabbit anti-phospho-AMPKα (Santa Cruz; 1:500), rabbit anti-AMPKα (Santa Cruz; 1:500), rabbit anti-lamin B1 (Santa Cruz; 1:500) and rabbit anti-Nrf2 (Santa Cruz; 1:500). Blots were detected with Alexa Fluor® 680 goat anti-rabbit IgG (Life technologies, UK) using Licor Odyssey. Equal protein loading was assessed using rabbit anti-actin antibody (Sigma, 1:1000).

2.5 Immunofluorescence microscopy

This was carried out as described elsewhere [9]. Immunofluorescence detection of rabbit anti-NF-κB p65 antibody (Santa Cruz; 1:100) was carried with Alexa Fluor 488-conjugated donkey anti rabbit IgG secondary antibody (Life Technologies; 1:500) and images obtained using EVOS® FLoid® cell imaging station.

2.6 DNA binding assays

DNA binding assays were used to determine the effects of OTBK on DNA binding of NF-κB and Nrf2 transcription factors in BV-2 microglia. Following cell treatment, nuclear extracts were prepared and assayed using the TransAM NF-κB and Nrf2 transcription factor EMSA kits (Activ Motif, Belgium) according to the manufacturer’s

instructions. The TransAM transcription factor assay kits employed a 96-well plate to which oligonucleotides containing the NF-κB consensus site (5'-GGGACTTTCC-3') or the ARE consensus binding site (5'-GTCACAGTGACTCAGCAGAATCTG-3') have been immobilised.

2.7 Statistical analyses

Values of all experiments were represented as a mean ± SEM of at least 3 independent experiments. Differences between values from different treatments were compared using one-way analysis of variance (ANOVA) followed by a post-hoc Tukey test.

3. Results and discussion

3.1 OTBK reduced the production of pro-inflammatory cytokines, NO/iNOS and PGE_2/COX-2 from LPS + IFNγ-stimulated BV-2 microglia without affecting cell viability

Analyses of BV-2 culture supernatants revealed that OTBK produced significant ($p<0.05$) reduction in the levels of pro-inflammatory TNFα (Figure 2A), IL-6 (Figure 2B), PGE_2 (Figure 2C) and nitrite (Figure 2D) in BV-2 microglia activated with LPS (100 ng/ml) and IFNγ (5 ng/ml). Furthermore, results of immunoblotting experiments in Figures 3A, 3B and 3C suggest that the compound reduced PGE_2 and nitrite production through inhibition of COX-2 and iNOS protein expression, respectively. These actions are consistent with those shown by natural compounds such as curcumin [15], and are similar to those earlier observed with tiliroside, which showed marked inhibition of neuroinflammation in BV-2 microglia by the compound [8, 9].

We also observed that treatment of BV-2 cells with 2.5, 5 and 10 µM OTBK followed by LPS + IFNγ stimulation for 24 h did not affect the viability of these cells, whereas higher concentrations (20 and 40 µM) of the compound produced significant ($p<0.001$) reduction in cell viability (Figures 4A and 4B). This clearly suggests that the compound was not cytototoxic at anti-inflammatory concentrations of 2.5, 5 and 10 µM. **Protective effect of OTBK in microglia conditioned media-induced neurotoxicity**

Having observed that OTBK inhibited inflammatory mediator release from LPS + IFNγ-activated BV-2 microglia, we were interested in determining whether this compound would prevent microglia-induced neurotoxicity in HT22 mouse hippocampal neurons. Results in Figure 5A show that exposure of HT22 cells to microglia conditioned media from cells stimulated with a combination of LPS and IFNγ resulted in significant ($p<0.001$) reduction in neuronal viability. Interestingly, incubation of conditioned media from BV-2 cells treated with OTBK (2.5-10 µM) prior to LPS and IFNγ stimulation resulted in significantly increased ($p<0.05$) number of viable neurons. In addition, there was a corresponding significant ($p<0.01$) increase in the generation of cellular ROS in neurons incubated with conditioned media from LPS and IFNγ only treated BV-2 microglia, while there was a reduction in ROS production when neurons were exposed to conditioned media from microglia treated with OTBK prior to LPS and IFNγ (Figure 5B). These results have confirmed that inhibition of neuroinflammation involving reactive microglia is a critical target in achieving neuroprotection in the treatment of neurodegenerative diseases [16]. Furthermore the activity of OTBK in preventing microglia-mediated neurotoxicity has been demonstrated.

3.3 OTBK inhibited NF-κB activation

It is now widely accepted that the production of pro-inflammatory mediators such as TNFα, IL-6 and expression of proteins like COX-2 and iNOS during neuroinflammation is regulated by the transcription factor NF-κB. We were therefore interested in establishing whether inhibition of NF-κB activation is a mechanism responsible for the anti-inflammatory activity of OTBK. Initial ELISA experiments demonstrated that the compound prevented the phosphorylation of p65 sub-unit of NF-κB, which is one of the critical steps in the microglia NF-κB activation pathway (Figure 6A). This was confirmed by results of immunofluorescence experiments which showed that OTBK prevented LPS + IFNγ-induced nuclear accumulation of NF-κB p65 sub-unit in BV-2 microglia (Figure 6B). Furthermore, DNA binding assays revealed that OTBK prevented LPS + IFNγ-induced DNA binding of NF-κB in BV-2 microglia (Figure 6C). Based on these results, we can conclude that OTBK inhibits neuroinflammation by modulating cellular activities resulting in the activation of NF-κB in a similar manner as the related compound, tiliroside.

3.4 Activation of AMPK in BV-2 microglia contributes to anti-inflammatory activity of OTBK

Based on reports demonstrating the effects of OTBK on glucose metabolism, studies showing activation of AMPK by a related compound [10, 11], as well as reported role of AMPK activation in neuroinflammation [4], we used immunoblotting to determine whether this compound could activate AMPKα in BV-2 microglia. We were also interested in evaluating the effect of OTBK on LPS + IFNγ-induced dephosphorylation of AMPK. Our results revealed that treatment of unstimulated BV-2 microglia with OTBK for 24 h resulted in significant ($p<0.05$) elevation in phospho-AMPKα protein in comparison with untreated control (Figure 7A). Separate experiments also revealed that stimulation of BV-2 microglia with a combination of LPS (100 ng/ml) and IFNγ (5 ng/ml) resulted in significant ($p<0.01$) suppression of phospho-AMPKα protein expression in comparison with control cells (Figure 7B). However, in the presence of OTBK (2.5-10 µM), there was a significant ($p<0.001$) reversal of LPS + IFNγ-induced inactivation of AMPK. This is an interesting outcome as studies have revealed a link between inflammation and dephosphorylation of AMPK in mice [17]. It therefore appears that reversal of inflammation-induced dephosphorylation of AMPK by OTBK and its anti-inflammatory activity are linked.

The role of AMPK activation in the anti-inflammatory activity of OTBK was then further investigated by treating BV-2 cells with potent and direct inhibitor of AMPK, dorsomorphin [18] (10 µM) followed by OTBK (10 µM) prior to LPS + IFNγ stimulation for 24 h. Analyses of culture supernatants showed that LPS + IFNγ stimulation resulted in a significant ($p<0.05$) elevation of TNFα and IL-6 levels, in comparison with control cells. Also, OTBK produced a characteristic reduction in the levels of these cytokines in BV-2 microglia stimulated with LPS + IFNγ. In cells treated with dorsomorphin (10 µM) prior to stimulation with LPS + IFNγ, there was no reduction in the production of these pro-inflammatory mediators, suggesting a lack of anti-inflammatory activity. However, inhibition of neuroinflammation as shown by reduction in TNFα (Figure 7C) and nitrite (Figure 7D) production by OTBK was diminished in the presence of dorsomorphin. The loss of anti-inflammatory activity in the presence of the AMPK antagonist further shows that inhibition of neuroinflammation by OTBK is related to its ability to activate AMPK. Some studies have suggested a role for AMPK as a negative regulator of inflammatory signalling

pathways in macrophages [19]. Taken together, our results appear to suggest that OTBK possibly targets mechanisms involved in negative regulation of inflammation by AMPK.

Other studies have linked anti-neuroinflammatory activity to activation of AMPK in BV-2 microglia [20], indicating that compounds which activate this kinase in the microglia may inhibit neuroinflammation [21]. An example of such a compound is thymoquinone found in cumin seed oil which was reported to inhibit neuroinflammation through mechanisms linked to AMPK and SIRT1 [22]. Similar activity has been reported for lycopene [23], hydrogen sulphide [24], caffeic acid phenethyl ester (CAPE) [25] and resveratrol [26].

3.5 Activation of Nrf2 by OTBK contributes to its anti-inflammatory activity in BV-2 microglia

Research reported by Zimmermann et al. [27] showed that there is a crosstalk between the AMPK and Nrf2/HO-1 signalling pathways and suggested that compounds like xanthohumol are able to induce dual activation of both pathways through mechanisms involving reduced endoplasmic reticulum stress. This led us to investigate whether OTBK would have any effect on Nrf2 activation in BV-2 microglia. In Figures 8A and 8B, we show that treatment with OTBK induced an increase in accumulation of Nrf2 in the nucleus in both unstimulated and LPS + IFNγ-stimulated BV-2 microglia. Results of DNA binding assays in Figure 8C show that there was significant ($p<0.05$) increase in the binding of Nrf2 to ARE consensus sites following treatment of BV-2 cells with OTBK (5 and 10 µM). Interestingly, at 2.5 µM, the compound did not produce significant effect on Nrf2 activity. Similarly, treatment of LPS + IFNγ-stimulated BV-2 cells with 5 and 10 µM of OTBK resulted in significant increase in DNA binding of Nrf2, while 2.5 µM of the compound did not produce a significant effect (Figure 8D).

Western blotting experiments revealed that treatment of unstimulated BV-2 microglia with 2.5 µM of OTBK did not produce significant increase in the downstream HO-1 protein (Figures 9A). On increasing the concentration of the compound to 5 and 10 µM, there was significant ($p<0.001$) increase in levels of HO-1 protein in BV-2 microglia. In LPS + IFNγ-stimulated cells however, significant increase in HO-1 protein was observed with 2.5-10 µM of OTBK, in comparison with either

unstimulated cells or with cells stimulated with LPS + IFNγ (Figure 9B). These results suggest that OTBK produces Nrf2-mediated increase in the levels of the antioxidant HO-1 protein.

Following results showing that OTBK activated Nrf2 in BV-2 microglia and based on our previous studies which demonstrated that anti-inflammatory activity of compounds such as tiliroside is dependent on Nrf2 [9, 14, 28], we used a known Nrf2 inhibitor, trigonelline to investigate whether OTBK would retain its anti-inflammatory activity in the presence of the inhibitor. Treatment of LPS + IFNγ stimulated BV-2 microglia with OTBK (10 μM) resulted in suppression of both TNFα and nitrite production, while anti-inflammatory activity was not observed when the cells were pre-treated with trigonelline (100 μM) prior to LPS + IFNγ stimulation. However, following treatment of LPS + IFNγ-activated BV-2 microglia with trigonelline (100 μM) prior to OTBK (10 μM) we observed that the anti-inflammatory effects of the compound on TNFα and nitrite production were partially reduced (Figures 10A and 10B). These results appear to suggest that inhibition of Nrf2 by trigonelline reduced the ability of OTBK to exert anti-inflammatory activity in BV-2 microglia. Several studies have reported that trigonelline is a potent inhibitor of Nrf2; experiments in cellular models have revealed that trigonelline interfered with Nrf2 activation, and suppressed induction of Nrf2/ARE-dependent gene expression [29-32]. Also, inhibition of Nrf2 by trigonelline in mice was shown to produce similar effects to Nrf2 knockout in attenuating hypertension, renal injury, as well as tubulointerstitial fibrosis [33]. Consequently, our results in BV-2 cells indicate that OTBK probably produces anti-inflammatory activity through mechanisms requiring activation of Nrf2.

Kaempferol and tiliroside, which are similar compounds to OTBK have been reported to produce inhibition of neuroinflammation in BV-2 microglia. For instance similar to OTBK, kaempferol has been reported to suppress LPS-induced nitric oxide production in BV-2 microglia [34-36]. It has been suggested that the anti-inflammatory effect of kaempferol on NO (as well as PGE_2, TNFα, IL-1β and ROS) production in LPS-stimulated BV-2 may be related to its modulatory effect on NF-κB activation and p38 MAPK, JNK and AKT phosphorylation [37]. However, unlike what was observed with OTBK, AMPK- and Nrf2-dependent anti-inflammatory activity in BV-2 microglia has not been reported for kaempferol. With regards to tiliroside however, we have earlier reported similar Nrf2-mediated anti-inflammatory

activity in BV-2 microglia (8, 9). However, unlike OTBK it is not yet known if its ability to inhibit neuroinflammation is related to activation of AMPK in the microglia.

4. Conclusions

Our study has demonstrated for the first time that 3-*O*-[(*E*)-(2-oxo-4-(p-tolyl)-but-3-en-1-yl] kaempferol inhibits neuroinflammation and neuroinflammation-mediated neurotoxicity. Furthermore, the compound produced activation of AMPKα and Nrf2 in BV-2 microglia which possibly contribute to its anti-inflammatory activity. These data suggest that 3-*O*-[(*E*)-(2-oxo-4-(p-tolyl) but-3-en-1-yl] kaempferol is a potential small molecule for preventing microglia-mediated inflammation.

References

1. B. Zhang, C. Gaiteri, L.G. Bodea, et al., Integrated systems approach identifies genetic nodes and networks in late-onset Alzheimer's disease, Cell 153 (2013) 707-720.
2. A. Trovato Salinaro, M. Pennisi, R. Di Paola, M. Scuto, R. Crupi, M.T. Cambria, et al., Neuroinflammation and neurohormesis in the pathogenesis of Alzheimer's disease and Alzheimer-linked pathologies: modulation by nutritional mushrooms, Immun Ageing 15 (2018) 8.
3. S. Vivekanantham, S. Shah, R. Dewji, A. Dewji, C. Khatri, R. Ologunde, Neuroinflammation in Parkinson's disease: role in neurodegeneration and tissue repair, Int J Neurosci 125 (2015) 717-725.
4. C.A. Peixoto, W.H. Oliveira, S.MD.R. Araújo, A.K.S. Nunes, AMPK activation: Role in the signaling pathways of neuroinflammation and neurodegeneration, Exp Neurol 298 (2017) 31-41.
5. C.C. Chen, J.T. Lin, Y.F. Cheng, C.Y. Kuo, C.F. Huang, S.H. Kao, et al., Amelioration of LPS-induced inflammation response in microglia by AMPK activation, Biomed Res Int 2014 (2014) 1-9.
6. A.T. Dinkova-Kostova, R.V. Kostov, A.G. Kazantsev, The role of Nrf2 signaling in counteracting neurodegenerative diseases, FEBS J 285 (2018) 3576-3590.
7. B.E. Townsend, R.W. Johnson, Sulforaphane induces Nrf2 target genes and attenuates inflammatory gene expression in microglia from brain of young adult and aged mice, Exp Gerontol 73 (2016) 42-48.
8. R. Velagapudi, M. Aderogba, O.A. Olajide, Tiliroside, a dietary glycosidic flavonoid, inhibits TRAF-6/NF-κB/p38-mediated neuroinflammation in activated BV2 microglia, Biochim Biophys Acta 1840 (2014) 3311-3319.
9. R. Velagapudi, A. El-Bakoush, O.A. Olajide, Activation of Nrf2 pathway contributes to neuroprotection by the dietary flavonoid tiliroside, Mol Neurobiol 55 (2018) 8103-8123.
10. N. Qin, C.B. Li, M.N. Jin, L.H. Shi, H.Q. Duan, W.Y. Niu, Synthesis and biological activity of novel tiliroside derivants, Eur J Med Chem 46 (2011) 5189-5195.
11. L. Shi, N. Qin, L. Hu, L. Liu, H. Duan, W. Niu, Tiliroside-derivatives enhance GLUT4 translocation via AMPK in muscle cells, Diabetes Res Clin Pract 92 (2011) e41-e46.

12. K.S. Babu, X.C. Li, M.R. Jacob, Q. Zhang, S.I. Khan, D. Ferreira, A.M. Clark, Synthesis, antifungal activity, and structure-activity relationships of coruscanone A analogues, J Med Chem 49 (2006) 7877-7886.
13. U.P. Okorji, O.A. Olajide, A semi-synthetic derivative of artemisinin, artesunate inhibits prostaglandin E2 production in LPS/IFNγ-activated BV2 microglia, Bioorg Med Chem 22 (2014) 4726-4734.
14. U.P. Okorji, R. Velagapudi, A. El-Bakoush, B.L. Fiebich, O.A. Olajide, Antimalarial drug artemether inhibits neuroinflammation in BV2 microglia through Nrf2-dependent mechanisms, Mol Neurobiol 53 (2016) 6426-6443.
15. A. Cianciulli, R. Calvello, C. Porro, T. Trotta, R. Salvatore, M.A. Panaro, PI3k/Akt signalling pathway plays a crucial role in the anti-inflammatory effects of curcumin in LPS-activated microglia, Int Immunopharmacol 36 (2016) 282-290.
16. N. Gresa-Arribas, C. Viéitez, G. Dentesano, J. Serratosa, J. Saura, C. Solà, Modelling neuroinflammation in vitro: a tool to test the potential neuroprotective effect of anti-inflammatory agents, PLoS One 7 (2012) e45227.
17. K. Fan, L. Lin, Q. Ai, J. Wan, J. Dai, G. Liu, L. Tang, Y. Yang, P. Ge, R. Jiang, L. Zhang, Lipopolysaccharide-induced dephosphorylation of AMPK-activated protein kinase potentiates inflammatory injury via repression of ULK1-dependent autophagy, Front Immunol. 9 (2018) 1464.
18. G. Zhou, R. Myers, Y. Li, Y. Chen, X. Shen, J. Fenyk-Melody, et al., Role of AMP-activated protein kinase in mechanism of metformin action, J Clin Invest 108 (2001)1167–1174.
19. D. Sag, D. Carling, R.D. Stout, J. Suttles, Adenosine 5'-monophosphate-activated protein kinase promotes macrophage polarization to an anti-inflammatory functional phenotype, J Immunol. 181 (2008) 8633-8641.
20. Y. Ma, J. Bu, H. Dang, J. Sha, Y. Jing, A.I. Shan-jiang, H. Li, Y. Zhu, Inhibition of adenosine monophosphate-activated protein kinase reduces glial cell-mediated inflammation and induces the expression of Cx43 in astroglias after cerebral ischemia, Brain Res 1605 (2015) 1-11.
21. Y. Wang, Y. Huang, Y. Xu, W. Ruan, H. Wang, Y. Zhang, et al., A Dual AMPK/Nrf2 activator reduces brain inflammation after stroke by enhancing microglia M2 polarization, Antioxid Redox Signal 28 (2018)141-163.

22. R. Velagapudi, A. El-Bakoush, I. Lepiarz, F. Ogunrinade, O.A. Olajide OA, AMPK and SIRT1 activation contribute to inhibition of neuroinflammation by thymoquinone in BV2 microglia, Mol Cell Biochem 435 (2017) 149-162.
23. H.Y. Lin, B.R. Huang, W.L. Yeh, C.H. Lee, S.S. Huang, C.H. Lai, H. Lin, D.Y. Lu, Antineuroinflammatory effects of lycopene via activation of adenosine monophosphate-activated protein kinase-α1/heme oxygenase-1 pathways, Neurobiol Aging 35 (2014) 191-202.
24. X. Zhou, Y. Cao, G. Ao, L. Hu, H. Liu, J. Wu, et al., CaMKKβ-dependent activation of AMP-activated protein kinase is critical to suppressive effects of hydrogen sulfide on neuroinflammation, Antioxid Redox Signal 21 (2014) 1741-1758.
25. C.F. Tsai, Y.H. Kuo, W.L. Yeh, C.Y. Wu, H.Y. Lin, S.W. Lai, et al., Regulatory effects of caffeic acid phenethyl ester on neuroinflammation in microglial cells, Int J Mol Sci 16 (2015) 5572-5589.
26. Y.J. Yang, L. Hu, X.P. Xia, C.Y. Jiang, C. Miao, C.Q. Yang, M. Yuan, L. Wang, Resveratrol suppresses glial activation and alleviates trigeminal neuralgia via activation of AMPK, J Neuroinflammation 13 (2016) 84.
27. K. Zimmermann, J. Baldinger, B. Mayerhofer, A.G. Atanasov, V.M. Dirsch, E.H. Heiss, Activated AMPK boosts the Nrf2/HO-1 signaling axis--A role for the unfolded protein response, Free Radic Biol Med 88 (2015) 417-426.
28. S.A. Onasanwo, R. Velagapudi, A. El-Bakoush, O.A. Olajide, Inhibition of neuroinflammation in BV2 microglia by the biflavonoid kolaviron is dependent on the Nrf2/ARE antioxidant protective mechanism, Mol Cell Biochem 414 (2016) 23-36.
29. U. Boettler, K. Sommerfeld, N. Volz, G. Pahlke, N. Teller, V. Somoza, R. Lang, T. Hofmann, D. Marko, Coffee constituents as modulators of Nrf2 nuclear translocation and ARE (EpRE)-dependent gene expression, J Nutr Biochem. 22 (2011) 426-440.
30. A. Arlt, S. Sebens, S. Krebs, C. Geismann, M. Grossmann, M.L. Kruse, S. Schreiber, H. Schäfer, Inhibition of the Nrf2 transcription factor by the alkaloid trigonelline renders pancreatic cancer cells more susceptible to apoptosis through decreased proteasomal gene expression and proteasome activity, Oncogene 32(2013) 4825-4835.

31. J.L. Roh, E.H. Kim, H. Jang, D. Shin, Nrf2 inhibition reverses the resistance of cisplatin-resistant head and neck cancer cells to artesunate-induced ferroptosis, Redox Biol. 11 (2017) 254-262.
32. S.E.G. van Raaij, R. Masereeuw, D.W. Swinkels, R.P.L. van Swelm, Inhibition of Nrf2 alters cell stress induced by chronic iron exposure in human proximal tubular epithelial cells, Toxicol Lett. 295 (2018) 179-186
33. S. Zhao, A. Ghosh, C.S. Lo, I. Chenier, J.W. Scholey, J.G. Filep, J.R. Ingelfinger, S.L. Zhang, J.S.D. Chan, Nrf2 deficiency upregulates intrarenal angiotensin-converting enzyme-2 and angiotensin 1-7 receptor expression and attenuates hypertension and nephropathy in diabetic mice, Endocrinology 159 (2018) 836-852.
34. Y.S. Kwon, S.S. Kim, S.J. Sohn, P.J. Kong, I.Y. Cheong, C.M. Kim, W. Chun, Modulation of suppressive activity of lipopolysaccharide-induced nitric oxide production by glycosidation of flavonoids, Arch Pharm Res. 27 (2004) 751-756.
35. M.K. Lee, H.Y. Jeon, K.Y. Lee, S.H. Kim, C.J. Ma, S.H. Sung, H.S. Lee, M.J. Park, Y.C. Kim, Inhibitory constituents of *Euscaphis japonica* on lipopolysaccharide-induced nitric oxide production in BV2 microglia, Planta Med. 73 (2007) 782-786.
36. N. Cho N, J.H. Choi, H. Yang, E.J. Jeong, K.Y. Lee, Y.C. Kim, S.H. Sung, Neuroprotective and anti-inflammatory effects of flavonoids isolated from *Rhus verniciflua* in neuronal HT22 and microglial BV2 cell lines, Food Chem Toxicol. 50 (2012) 1940-1945.
37. S.E. Park, K. Sapkota, S. Kim, H. Kim, S.J. Kim, Kaempferol acts through mitogen-activated protein kinases and protein kinase B/AKT to elicit protection in a model of neuroinflammation in BV2 microglial cells, Br J Pharmacol. 164 (2011) 1008-1025.

Figure Legends

Figure 1

Structure of OTBK

Figure 2

OTBK reduced levels of TNFα (A), IL-6 (B), PGE_2 (C) and nitrite (D) in culture supernatants of BV-2 microglia stimulated with LPS (100 ng/ml) and IFNγ (5 ng/ml) for 24 h. All values are expressed as mean ± SEM for three independent experiments. Data were analysed using one-way ANOVA for multiple comparisons with post-hoc Tukey test. *p<0.05, **p<0.01, ***p<0.001 in comparison with LPS/ IFNγ control.

Figure 3

Inhibition of LPS/ IFNγ-induced increase in protein levels of COX-2 and iNOS in BV-2 microglia by OTBK. Cultured cells were treated with OTBK prior to stimulation with LPS (100 ng/ml) and IFNγ (5 ng/ml) for 24 h. Cell lysates were immunoblotted using COX-2 and iNOS antibodies (A). Densitometric analyses of three independent experiments are shown for COX-2 (B) and iNOS (C). Data were analysed using one-way ANOVA for multiple comparisons with post-hoc Tukey test. *p<0.05, **p<0.01, ***p<0.001 in comparison with LPS/ IFNγ control.

Figure 4

Treatment of BV-2 microglia with OTBK (2.5, 5 and 10 µM), followed by stimulation with LPS (100 ng/ml) and IFNγ (5 ng/ml) for 24 h did not reduce cell viability. Data were analysed using one-way ANOVA for multiple comparisons with post-hoc Tukey test. ***p<0.001 in comparison with untreated control.

Figure 5

Protection against microglia-induced neuronal damage by OTBK. HT22 neurons were incubated with conditioned culture medium obtained from BV-2 microglia that were stimulated with LPS and IFNγ for 24 h (A). MTT assay revealed an increase in HT22 viability in cells treated with OTBK, in comparison with control. OTBK treatment caused a reduction in cellular ROS generation in HT22 cells (B). Data

were analysed using one-way ANOVA for multiple comparisons with post-hoc Tukey test. *p<0.05, **p<0.01, ***p<0.001 in comparison with LPS/ IFNγ stimulation.

Figure 6

OTBK suppresses neuroinflammation by interfering with NF-κB activity through inhibition of p65 phosphorylation (A), nuclear accumulation of p65 sub-unit of NF-κB (B) and inhibition of DNA binding of NF-κB (C) in BV-2 cells stimulated with LPS (100 ng/ml) and IFNγ (5 ng/ml). Data were analysed using one-way ANOVA for multiple comparisons with post-hoc Tukey test. **p<0.01, ***p<0.001 in comparison with LPS/ IFNγ or TNFα stimulation.

Figure 7A & 7B

OTBK directly increased levels of phospho-AMPKα in BV-2 microglia following incubation for 24 h (A), and reversed dephosphorylation of AMPKα induced by stimulation with LPS (100 ng/ml) and IFNγ (5 ng/ml) for 24 h (B). Cell lysates were analysed using immunoblotting for phospho-AMPKα and total AMPKα. Representative blots and densitometric analyses of three independent experiments are shown (Mean ± SEM; **p<0.01, ***p<0.001; one way ANOVA for multiple comparisons with post-hoc Tukey test).

Figure 7C & 7D

Inhibition of neuroinflammation by OTBK was diminished in the presence of dorsomorphin. BV-2 cells were treated with either OTBK (10 μM) and LPS (100 ng/ml) + IFNγ (5 ng/ml), dorsomorphin (10 μM) and LPS (100 ng/ml) + IFNγ (5 ng/ml), or dorsomorphin (10 μM), followed by OTBK (10 μM) and LPS (100 ng/ml) + IFNγ (5 ng/ml) for 24 h. Cells were analysed for TNFα (C) and nitrite (D). Data were analysed using one-way ANOVA for multiple comparisons with post-hoc Tukey test. ***p<0.001; untreated control versus LPS/ IFNγ stimulation. $^{\theta\theta}$p<0.01; OTBK + LPS + IFNγ treatment versus LPS + IFNγ only. $^{\&}$p<0.05; dorsomorphin + OTBK + LPS/IFNγ treatment compared with OTBK + LPS/ IFNγ treatment (n=6).

Figure 8

OTBK (5 and 10 μM) treatment significantly increased nuclear Nrf2 in the absence (A) and presence of LPS + IFNγ stimulation (B) in BV-2 microglia. Nuclear extracts

were analysed using immunoblotting for Nrf2 and lamin B. Representative blots and densitometric analyses of 3 independent experiments are shown. OTBK (5 and 10 µM) treatment without (C) and with LPS + IFNγ stimulation (D) increased DNA binding of Nrf2 to immobilised ARE consensus binding site in BV-2 microglia. Values are mean ± SEM; *p<0.05, **p<0.01, ***p<0.001; one way ANOVA for multiple comparisons with post-hoc Tukey test).

Figure 9

OTBK (5 and 10 µM) treatment significantly increased HO-1 protein in the absence (A) and presence of LPS + IFNγ stimulation (B) in BV-2 microglia. Representative blots and densitometric analyses of 3 independent experiments are shown (Mean ± SEM; ***p<0.001; one way ANOVA for multiple comparisons with post-hoc Tukey test).

Figure 10

Inhibition of neuroinflammation by OTBK was diminished in the presence of trigonelline. BV-2 cells were treated with either OTBK (10 µM) and LPS (100 ng/ml) + IFNγ (5 ng/ml), trigonelline (100 µM) and LPS (100 ng/ml) + IFNγ (5 ng/ml), or trigonelline (100 µM), followed by OTBK (10 µM) and LPS (100 ng/ml) + IFNγ (5 ng/ml) for 24 h. Cells were analysed for TNFα (A) and nitrite (B). Data were analysed using one-way ANOVA for multiple comparisons with post-hoc Tukey test. ***p<0.001; untreated control versus LPS/ IFNγ stimulation. $^{\theta\theta\theta}$p<0.001; OTBK + LPS + IFNγ treatment versus LPS + IFNγ only. $^{\&}$p<0.05; trigonelline + OTBK + LPS/IFNγ treatment compared with OTBK + LPS/ IFNγ treatment (n=6).

.

Figure 1

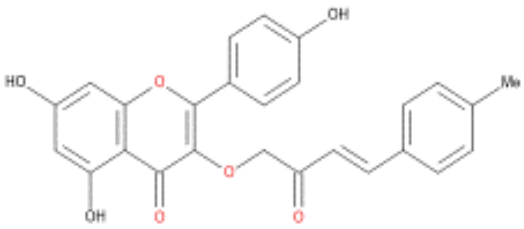

Figure 2

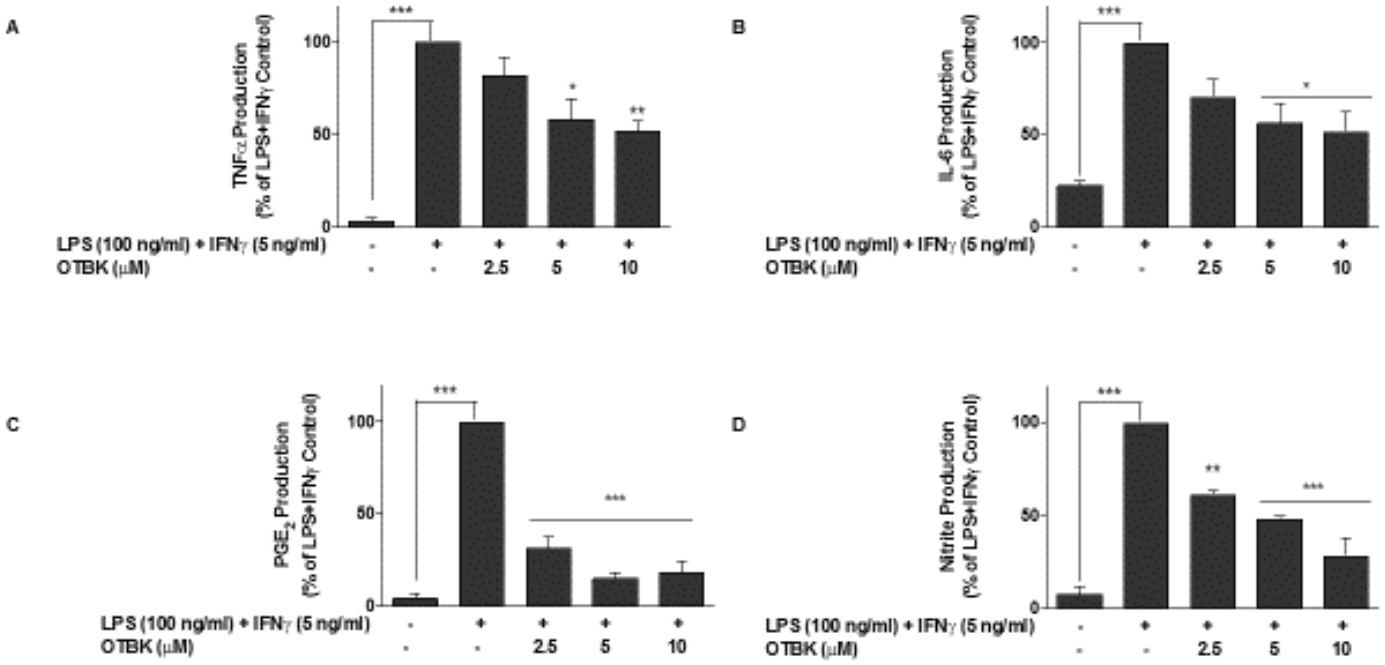
A
TNFα Production
(% of LPS+IFNγ Control)
100
50
0
***
*
**
LPS (100 ng/ml) + IFNγ (5 ng/ml) - + + + +
OTBK (μM) - - 2.5 5 10
B
IL-6 Production
(% of LPS+IFNγ Control)
100
50
0
***
*
LPS (100 ng/ml) + IFNγ (5 ng/ml) - + + + +
OTBK (μM) - - 2.5 5 10
C
PGE2 Production
(% of LPS+IFNγ Control)
100
50
0
***
***
LPS (100 ng/ml) + IFNγ (5 ng/ml) - + + + +
OTBK (μM) - - 2.5 5 10
D
Nitrite Production
(% of LPS+IFNγ Control)
100
50
0
***
**
***
LPS (100 ng/ml) + IFNγ (5 ng/ml) - + + + +
OTBK (μM) - - 2.5 5 10

Figure 3

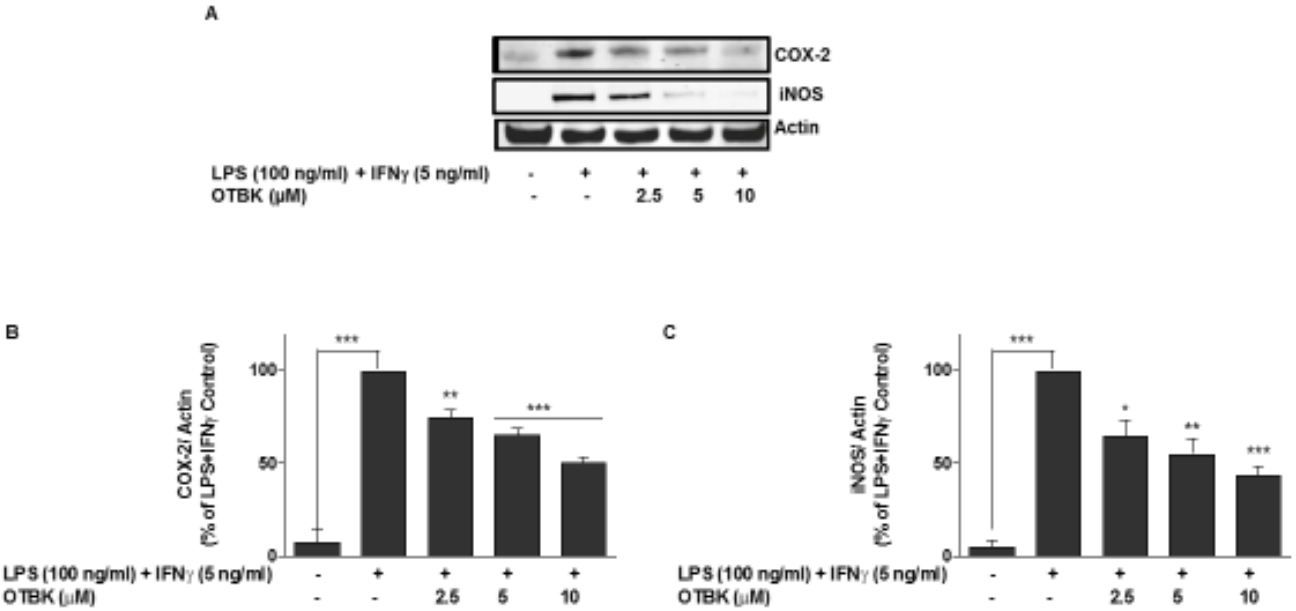
A
COX-2
iNOS
Actin
LPS (100 ng/ml) + IFNγ (5 ng/ml) - + + + +
OTBK (μM) - - 2.5 5 10
B
COX-2/ Actin
(% of LPS+IFNγ Control)
100
50
0
***
**
***
LPS (100 ng/ml) + IFNγ (5 ng/ml) - + + + +
OTBK (μM) - - 2.5 5 10
C
iNOS/ Actin
(% of LPS+IFNγ Control)
100
50
0
***
*
**
***
LPS (100 ng/ml) + IFNγ (5 ng/ml) - + + + +
OTBK (μM) - - 2.5 5 10

Figure 4

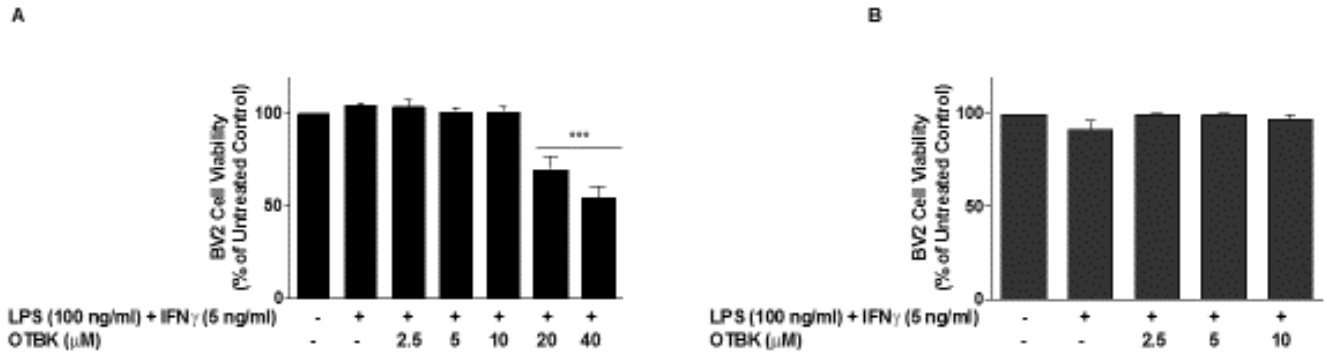
A
B
BV2 Cell Viability
(% of Untreated Control)
100
50
0
***
LPS (100 ng/ml) + IFNγ (5 ng/ml)
OTBK (μM)
- + + + + + +
- - 2.5 5 10 20 40
- + + + +
- - 2.5 5 10

Figure 5

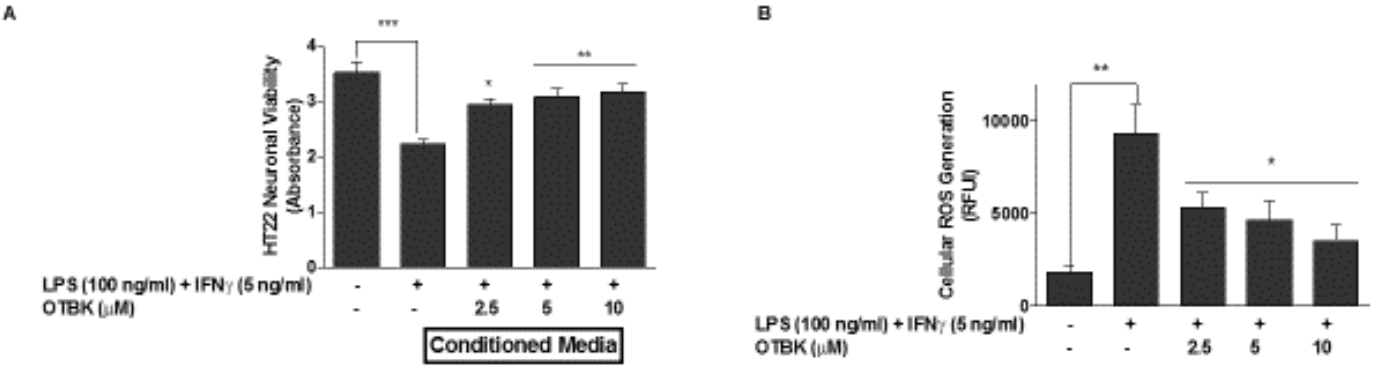
A
HT22 Neuronal Viability (Absorbance)
0
1
2
3
4
***
*
**
LPS (100 ng/ml) + IFNγ (5 ng/ml) - + + + +
OTBK (μM) - - 2.5 5 10
Conditioned Media
B
Cellular ROS Generation (RFU)
0
5000
10000
**
*
LPS (100 ng/ml) + IFNγ (5 ng/ml) - + + + +
OTBK (μM) - - 2.5 5 10

Figure 6

A

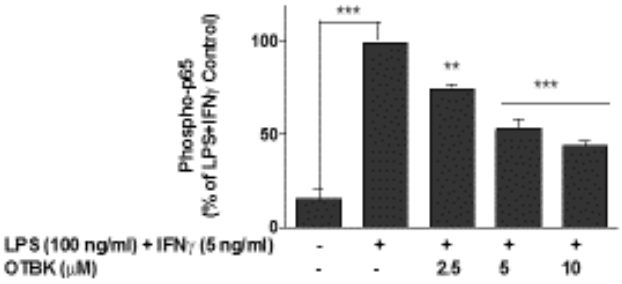
Phospho-p65
(% of LPS+IFNγ Control)
100
50
0
***
**
***
LPS (100 ng/ml) + IFNγ (5 ng/ml) - + + + +
OTBK (μM) - - 2.5 5 10

Figure 6

B

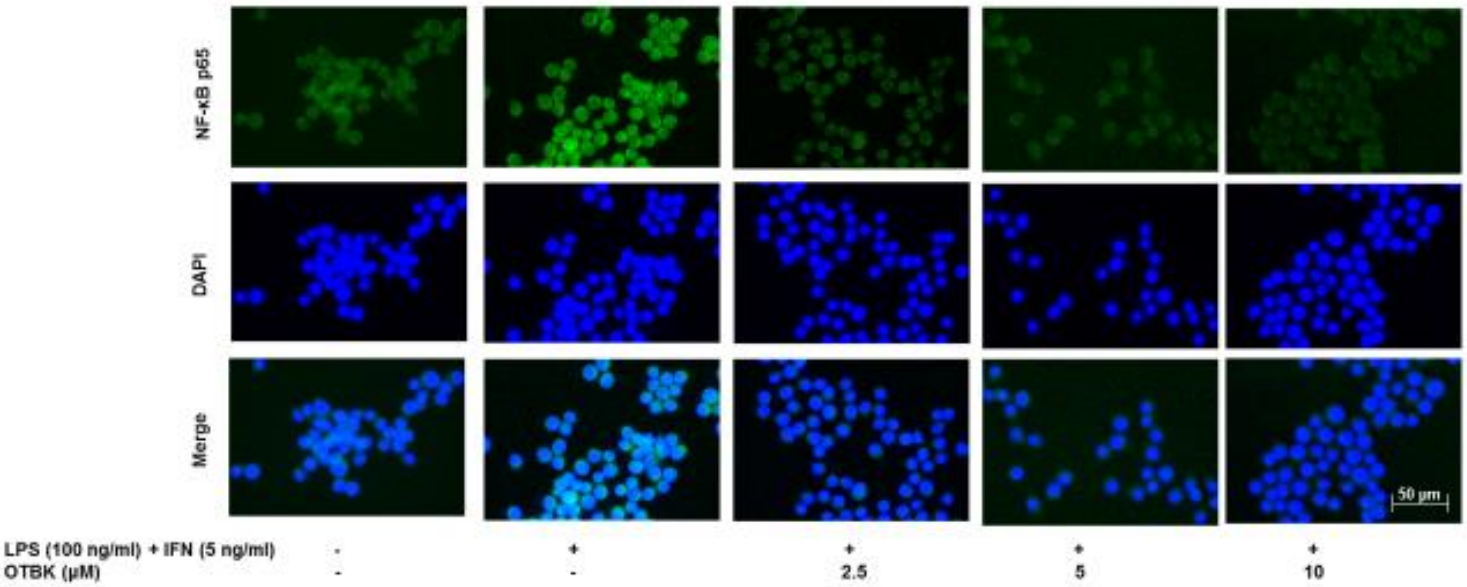

Figure 6

C

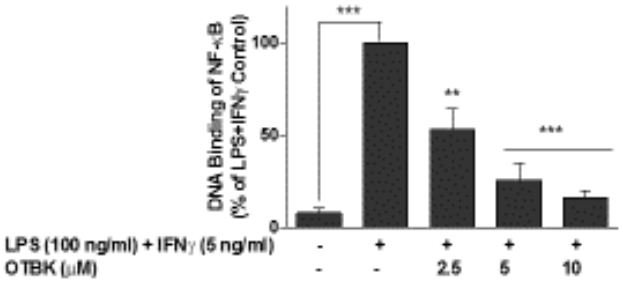
DNA Binding of NF-κB
(% of LPS+IFNγ Control)
100
50
0
***
**
***
LPS (100 ng/ml) + IFNγ (5 ng/ml)
OTBK (μM)
- + + + +
- - 2.5 5 10

Figure 7

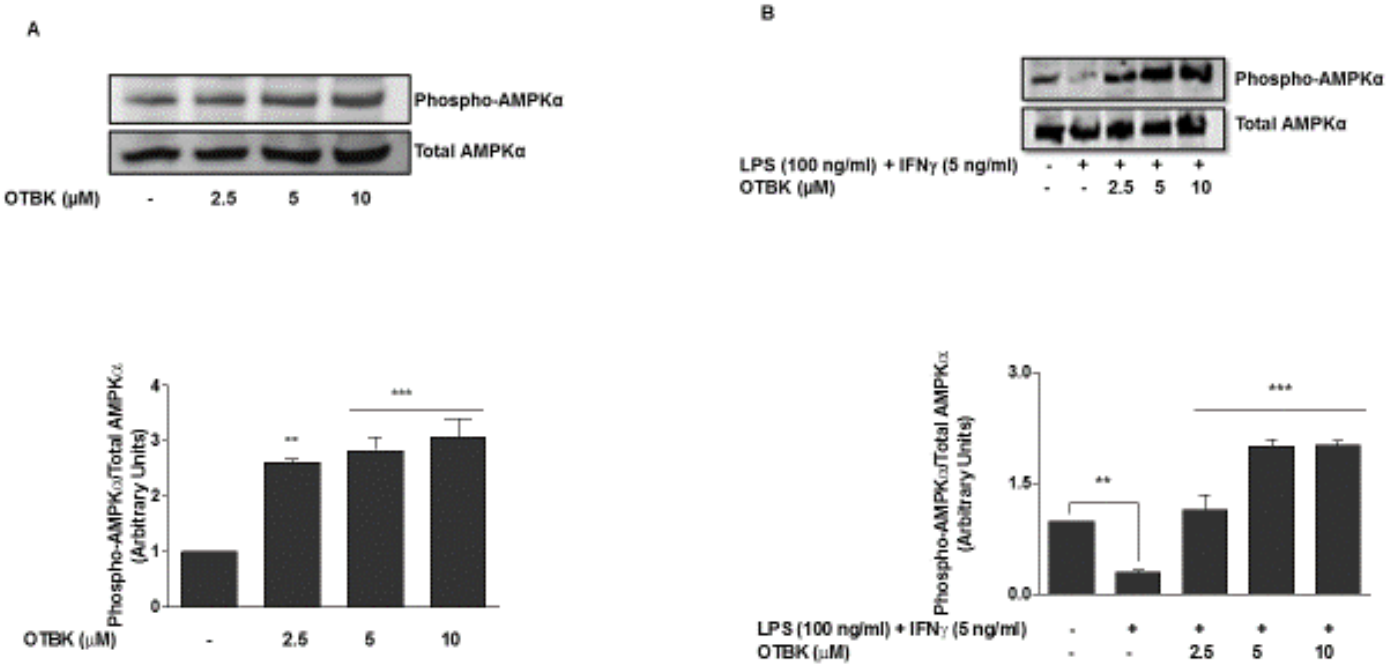
A
Phospho-AMPKα
Total AMPKα
OTBK (μM) - 2.5 5 10
Phospho-AMPKα/Total AMPKα (Arbitrary Units)
0
1
2
3
4
**
***
OTBK (μM) - 2.5 5 10
B
Phospho-AMPKα
Total AMPKα
LPS (100 ng/ml) + IFNγ (5 ng/ml) - + + + +
OTBK (μM) - - 2.5 5 10
Phospho-AMPKα/Total AMPKα (Arbitrary Units)
0.0
1.5
3.0
**
***
LPS (100 ng/ml) + IFNγ (5 ng/ml) - + + + +
OTBK (μM) - - 2.5 5 10

Figure 7

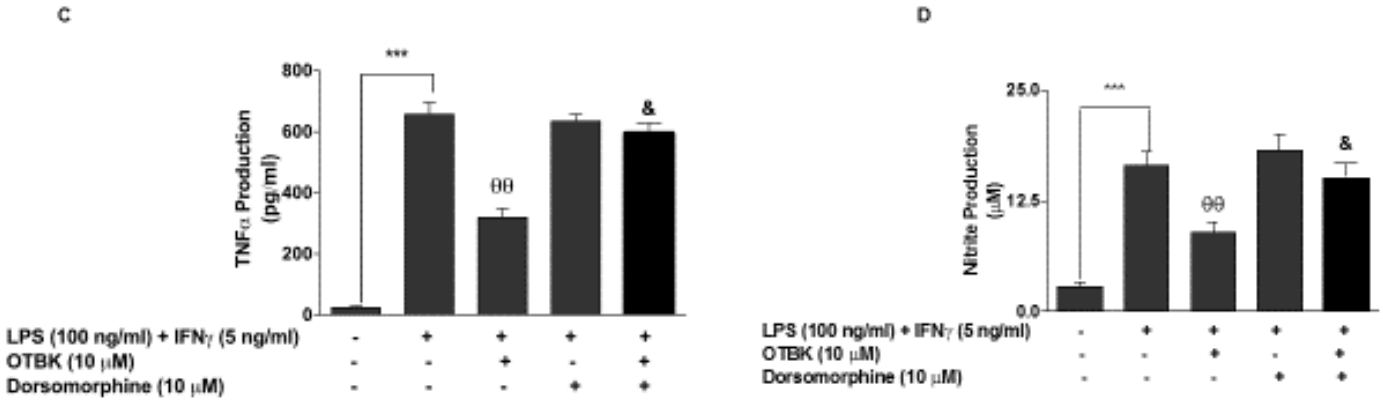
C
TNFα Production (pg/ml)
800
600
400
200
0
***
θθ
&
LPS (100 ng/ml) + IFNγ (5 ng/ml) - + + + +
OTBK (10 μM) - - + - +
Dorsomorphine (10 μM) - - - + +
D
Nitrite Production (μM)
25.0
12.5
0.0
***
θθ
&
LPS (100 ng/ml) + IFNγ (5 ng/ml) - + + + +
OTBK (10 μM) - - + - +
Dorsomorphine (10 μM) - - - + +

Figure 8

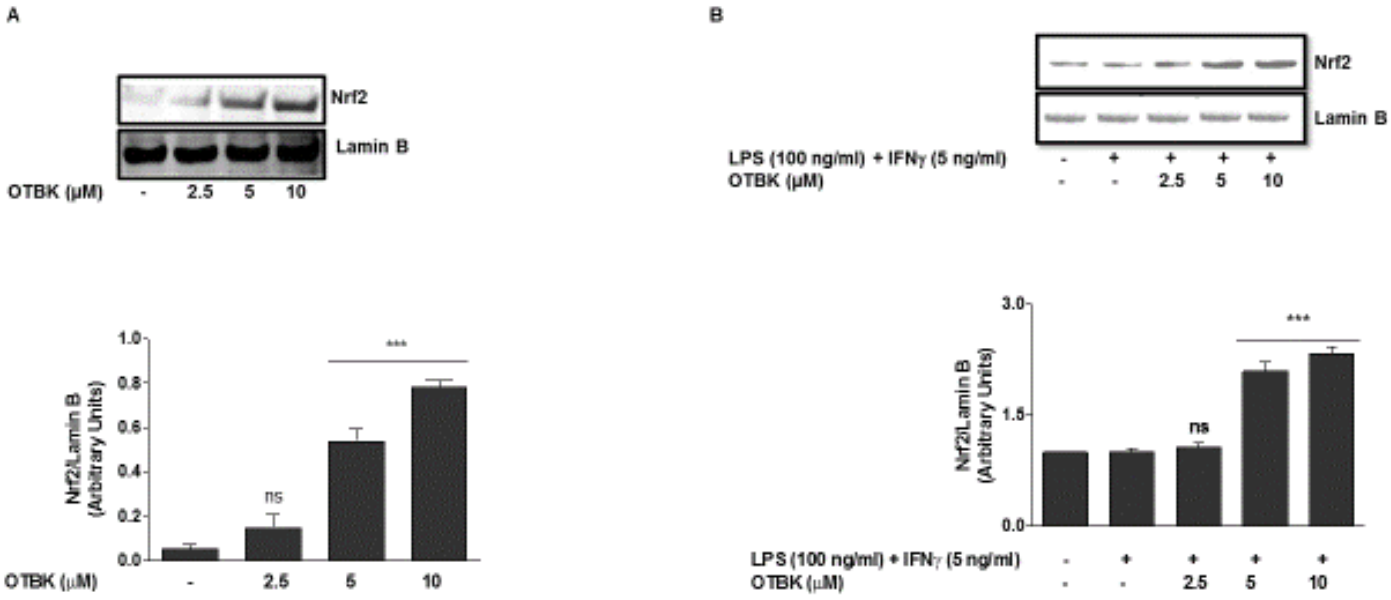
A
Nrf2
Lamin B
OTBK (μM) - 2.5 5 10
Nrf2/Lamin B (Arbitrary Units)
1.0
0.8
0.6
0.4
0.2
0.0
ns
***
OTBK (μM) - 2.5 5 10
B
Nrf2
Lamin B
LPS (100 ng/ml) + IFNγ (5 ng/ml) - + + + +
OTBK (μM) - - 2.5 5 10
Nrf2/Lamin B (Arbitrary Units)
3.0
1.5
0.0
ns
***
LPS (100 ng/ml) + IFNγ (5 ng/ml) - + + + +
OTBK (μM) - - 2.5 5 10

Figure 8

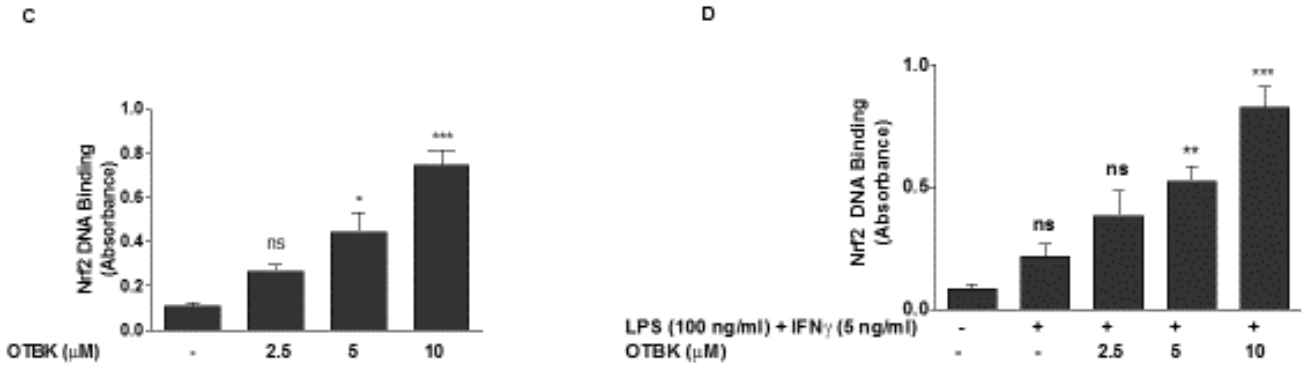
C
Nrf2 DNA Binding (Absorbance)
1.0
0.8
0.6
0.4
0.2
0.0
ns
*
***
OTBK (μM)
-
2.5
5
10
D
Nrf2 DNA Binding (Absorbance)
1.0
0.5
0.0
ns
ns
**
***
LPS (100 ng/ml) + IFNγ (5 ng/ml)
-
+
+
+
+
OTBK (μM)
-
-
2.5
5
10

Figure 9

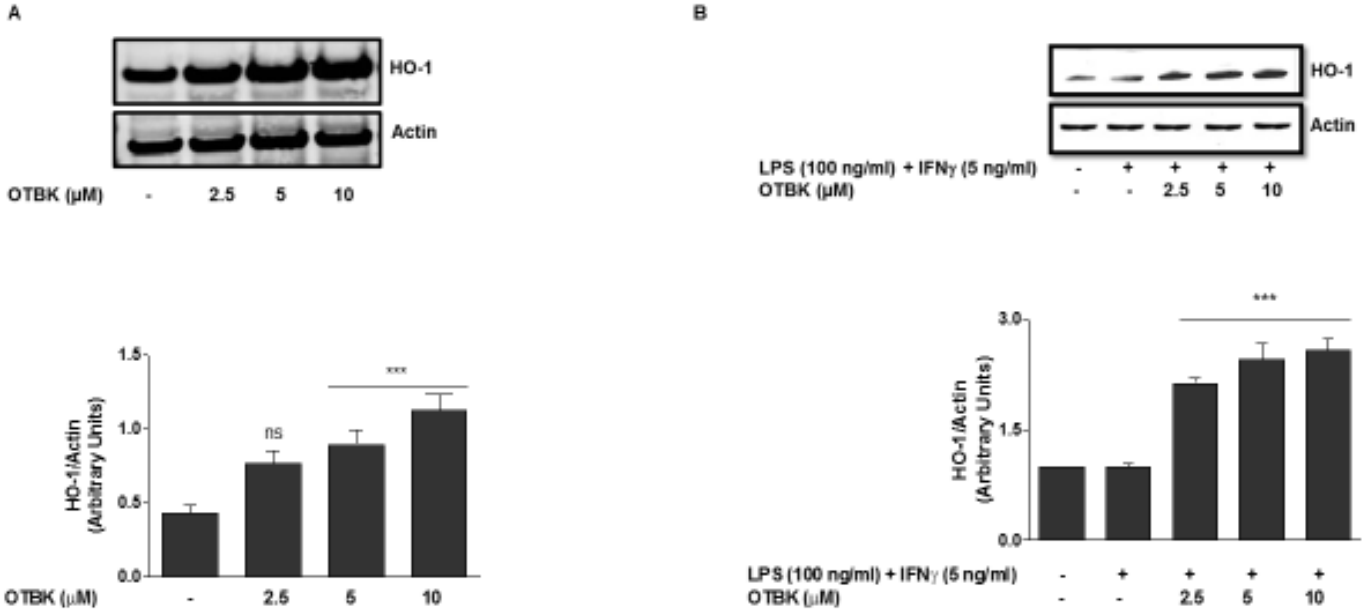
A
HO-1
Actin
OTBK (μM) - 2.5 5 10
HO-1/Actin (Arbitrary Units)
1.5
1.0
0.5
0.0
ns
***
OTBK (μM) - 2.5 5 10
B
HO-1
Actin
LPS (100 ng/ml) + IFNγ (5 ng/ml) - + + + +
OTBK (μM) - - 2.5 5 10
***
3.0
1.5
0.0
HO-1/Actin (Arbitrary Units)
LPS (100 ng/ml) + IFNγ (5 ng/ml) - + + + +
OTBK (μM) - - 2.5 5 10

Figure 10

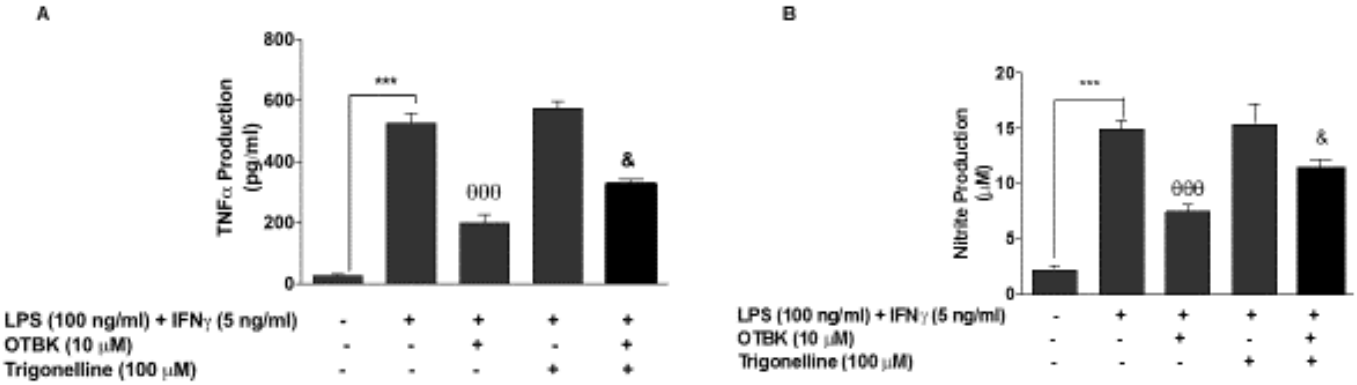
A
TNFα Production (pg/ml)
800
600
400
200
0
***
θθθ
&
LPS (100 ng/ml) + IFNγ (5 ng/ml) - + + + +
OTBK (10 μM) - - + - +
Trigonelline (100 μM) - - - + +
B
Nitrite Production (μM)
20
15
10
5
0
***
θθθ
&
LPS (100 ng/ml) + IFNγ (5 ng/ml) - + + + +
OTBK (10 μM) - - + - +
Trigonelline (100 μM) - - - + +

Supplementary Data 1

(*E*)-1-Bromo-4-(*p*-tolyl)but-3-en-2-one

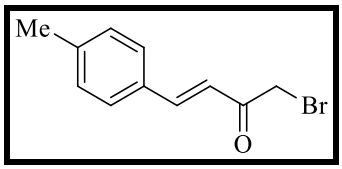

To a stirred solution of (*E*)-4-(*p*-tolyl)but-3-en-2-one (1.02 g; 6.25 mmol) in dry tetrahydrofuran (60 mL), was added slowly pyrrolidone hydrotribromide (3.71 g; 7.49 mmol) at room temperature over 1 h under an inert N_2 atmosphere. The reaction mixture was left to stir for 24 h. After this time, excess pyrrolidone hydrotribromide was removed by filtration and the filtrate was evaporated under reduced pressure. The resulting residue was dissolved in diethyl ether (20 mL) and then washed with brine (15 mL × 2). The organic layer was dried ($MgSO_4$) and then solvents were removed by rotary evaporation under reduced pressure. The crude product was purified by flash silica chromatography (ethyl acetate: petroleum ether, 2:1), affording the title compound as a yellow solid (0.9 g, 61 %, R_f = 0.29). Melting point: 94-95 ºC.

^{1}H NMR (400 MHz, $CDCl_3$) δ ppm 7.69 (1H, d, *J* = 16.1 Hz, C<u>H</u>=CH), 7.49 (2H, d, *J* = 7.8 Hz, Ar), 7.23 (2H, d, *J* = 7.8 Hz, Ar), 6.91 (1H, d, *J* = 16.1 Hz, CH=C<u>H</u>), 4.10 (C<u>H</u>$_2$), 2.40 (C<u>H</u>$_3$).

^{13}C NMR (100 MHz, $CDCl_3$) δ ppm 191.0 (C=O), 145.5 (CH), 141.8 (C), 131.2 (C), 129.8 (CH), 128.7 (CH), 121.3 (CH), 33.2 (CH_2), 21.6 (CH_3).

IR (neat) υ_{max} 2983, 2933, 1685, 1667, 1564, 1511, 1386, 1326, 1182, 1153, 1063, 976, 891, 860, 840, 710, 643, 517.

Previously reported.

3-*O*-[(*E*)-(2-Oxo-4-(*p*-tolyl)but-3-en-1-yl] kaempferol.

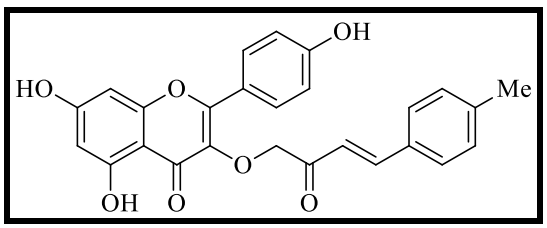

To a solution of kaempferol (0.025 g; 0.09 mmol) in dry 1,4-dioxane (4 mL), was added potassium carbonate (0.013 g; 0.09 mmol) and the mixture was heated at

reflux under an N_2 atmosphere at 80 ºC for 1.5 h. After this time, a solution of (*E*)-1-bromo-4-(*p*-tolyl)but-3-en-2-one (0.04 g; 0.15 mmol) in 1,4-dioxane (2 mL) was added drop-wise to the reaction mixture over 5 minutes and the reaction mixture was heated at 80ºC for 48 h. The solvents were removed by rotary evaporation under reduced pressure. The crude product was purified by flash silica chromatography (dichloromethane/ methanol; 10:1), affording the title compound as a yellow solid (0.013 g, 34 %, R_f = 0.36).

^{1}H NMR (400 MHz, CD_3OD-d_4) δ ppm 8.01 (2H, d, *J* = 8.7 Hz, Ar), 7.68 (1H, d, *J* = 16.1 Hz, C<u>H</u>=CH), 7.55 (O<u>H</u>), 7.53 (O<u>H</u>), 7.51 (O<u>H</u>), 7.47 (1H, d, *J* = 8.0 Hz, Ar), 7.25 (2H, d, *J* = 8.0 Hz. Ar), 6.97 (2H, d, *J* = 16.1 Hz, CH=C<u>H</u>), 6.88 (2H, d, *J* = 8.7 Hz, Ar), 6.39 (1H, d, *J* = 1.8 Hz, Ar), 6.18 (1H, d, *J* = 1.8 Hz, Ar), 5.10 (2H, s, C<u>H</u>$_2$), 2.35 (3H, s, C<u>H</u>$_3$).

^{13}C NMR (100 MHz, $CDCl_3$) δ ppm 195.6 (C), 178.0 (C), 164.5 (C), 161.7 (C), 160.4 (C), 156.9 (C), 156.3 (C), 143.9 (CH), 141.3 (C), 136.5 (C), 131.6 (C), 130.4 (CH), 129.3 (CH), 128.4 (CH), 121.1 (C), 120.5 (CH), 115.1 (CH), 104.4 (C), 98.4 (CH), 93.4 (CH), 75.2 (CH_2), 20.1 (CH_3).

MS $(ES)^+$: m/z [M - H] 443.2.

HRMS: [M] for $C_{26}H_{20}O_7$ calculated 444.1209, found 444.1204.

Previously reported (Qin et al., 2011).

Graphical Abstract